THE JOURNAL OF PHYSICAL CHEMISTRY B

Article

pubs.acs.org/JPCB

The Effect of Oxygen Heteroatoms on the Single Molecule Conductance of Saturated Chains

Emil Wierzbinski, Xing Yin, Keith Werling, and David H. Waldeck*

Department of Chemistry, University of Pittsburgh, Pittsburgh, Pennsylvania 15260, United States

Supporting Information

ABSTRACT: Single molecule conductance measurements on alkanedithiols and alkoxydithiols (dithiolated oligoethers) were performed using the STM-controlled break junction method in order to ascertain how the oxygen heteroatoms in saturated linear chains impact the molecular conductance. The experimental results show that the difference in conductance increases with chain length, over the range studied. Comparisons with electronic structure calculations and previous work on alkanes indicate that the conductance of the oligoethers is lower than that of alkane chains with the same length. Electronic structure calculations allow the difference in the conductance of these two families of molecules to be traced to differences in the spatial distribution of the molecular orbitals that contribute most to the conductance. A pathway analysis of the electronic coupling through the chain is used to explain how the difference in conductance between the alkane and oligoether molecules depends on the chain length.

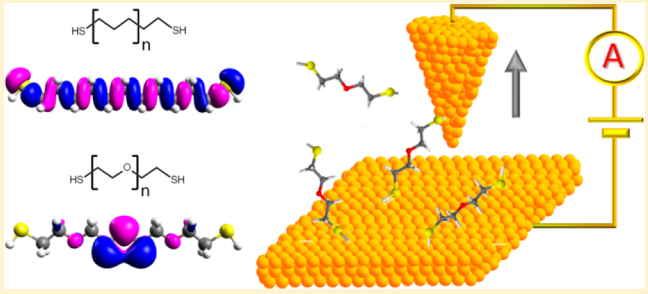

INTRODUCTION

Since the concept of molecular electronics first appeared,[1] progress in the development of experimental methods for determining the charge transfer properties of organic molecules (as prospective elements of electronic devices) has evolved to allow measurements on individual molecules.[2] Single molecule conductance measurements have been used to quantify the charge transport properties for a diverse array of molecules, including saturated and unsaturated hydrocarbons,[2d,3] conjugated oligomers,[4] fullerenes,[5] metal complexes,[6] porphyrins,[7] peptides,[8] and nucleic acids.[2b,9] Saturated hydrocarbons are often used as model molecular bridges,[3] because of the simplicity of their chemical structure and the establishment of superexchange as the charge transfer mechanism for chains of 20 methylenes and less. This work compares the conductance of methylene chains ($-CH_2-CH_2-CH_2$) to oligoethers ($-CH_2-CH_2-O-$) of corresponding length. The STM-controlled break junction method[2d] is used to measure the single molecule conductance of three alkanedithiols, containing 5, 8, and 11 methylene units, and the 3 corresponding dithiolated oligoethers, in which every third methylene unit is replaced by an oxygen. Comparison of these two sets of organic compounds provides a way to probe how the local electronic changes, between carbon and oxygen, affect the conductance of saturated chains. Presumably, the construction of molecular electronic devices will require binding several molecules or functional groups together, so that knowledge about the influence of various kinds of chemical bonds on the charge transfer properties is necessary in order to produce functional electrical circuits. Similar concerns were addressed recently by Whitesides and co-workers, who studied the impact of introducing amide bonds into hydrocarbon chains on the conductance through self-assembled monolayers (SAMs).[10] We report here that the conductance of the saturated chains can be decreased below the level found for saturated hydrocarbon chains and that an ether-type linkage may be used as an alternative to hydrocarbons in situations where one wishes to decrease the electronic coupling between different fragments of a complex molecular structure.

Comparison of the charge transfer properties of saturated hydrocarbon and ether chains has been probed electrochemically by Napper et al. using electroactive SAMs[11] and by Cheng et al.[12] using insulating films in contact with a redox couple. Both studies reported that the ether chains are more insulating, i.e., slower charge transfer rate, than alkane chains. Napper used alkanethiol and alkoxythiol SAMs, in which a small fraction (ca. 5%) of the chains were appended with a terminal ferrocene as a redox reporter group, and measured the electrochemical rate constant. They reported a four- to five-fold decrease in the rate constant for the ether-linked ferrocene as compared to the alkyl linked ferrocene. The electrochemical rate constant is sensitive to a combination of the properties of the molecular bridge, as well as the quality of the monolayer[13] and intermolecular interactions.[11,13a,14] Napper's study also varied the diluent molecules between the ferrocenated alkanethiols and alkoxythiols in order to quantify the influence of the electrical dipole in the monolayer on the measured rate constant. They found

Special Issue: Paul F. Barbara Memorial Issue

Received: August 8, 2012
Revised: October 26, 2012
Published: October 26, 2012

that 30−40% lower rate constants were measured whenever ferrocenated molecules with the same covalent linkage to the electrode were embedded in the ether monolayer. These studies showed that the effects produced by the environment (overall dipole moment in the monolayer) were dramatically smaller than the through-bond electronic coupling in determining the electrochemical rate constant.[15] The electrochemical through-bond unimolecular rate constant has been predicted to be proportional to the molecular conductance of the same molecular bridge;[16] thus, Napper's results imply that the single molecule conductances of alkanes should be higher than those of ethers.

In contrast to the electrochemical findings, Scullion et al. have reported an opposite trend for the single molecule conductance of ether and alkane chains, which they measured using the STM $I(s)$ method.[17] In this study, we use the STM break junction method to probe the molecular conductance for these two types of chains. While the magnitudes of the conductances reported here are found to be similar to those of Scullion et al., the interpretation of the results is different. It is widely appreciated that the conductance measured for molecules can be affected significantly by the binding motif between the molecule and the metal electrode (contacts); thus, the conclusions arising from the comparison between measurements on thiol-terminated molecules may be jeopardized.[3e,18] In addition, the working conditions in the two experiments could give rise to different solvation conditions and different conformations for the molecules between the two experiments, and other studies have shown that such differences can affect the measured conductances.[19] In the current study, we combine the experimental results with computational studies to conclude that the ether chains have a lower conductance than the alkane chains.

To understand the origin of the differences in the experimental conductance of the hydrocarbon and oligoether chains, computational studies are used to probe how the conductance changes in these molecules. To quantify the degree of the delocalization of the molecular orbitals (MOs), the concept of normalized localization factors is introduced, and it shows a higher delocalization of the MOs for the hydrocarbon chains than for the ether-linked chains. Assuming that more delocalization implies higher conductance, the trend in the delocalization level of the calculated MOs in these two families of molecules suggests that the single molecule conductance of the alkane is larger than that of the ether. In order to better understand the role of the oxygen atoms in the saturated chains, an analysis of electronic coupling pathways based on natural bond orbitals (NBO) is used.[11,20] A perturbation treatment[21] is used to assess the relative contribution from each pathway to the overall coupling, in the limits of hole-mediated superexchange and electron-mediated superexchange. This procedure shows that non-nearest neighbor couplings are a dominant contributor to the overall coupling for long chains. To understand the impact of the oxygen on the electronic coupling (and in consequence on the molecular conductance) and its length dependence, the pool of the orbital interactions used in the perturbation treatment is expanded to accommodate additional electronic interactions that arise from the presence of multiple oxygen atoms in the oligoether chains. This analysis shows how the oxygen atoms affect the electronic couplings differently in the short and long molecular chains.

EXPERIMENTAL SECTION

Compounds. The STM break junction method was used to measure the conductance of three alkoxy dithiolated saturated linear molecules [2-mercaptoethyl ether (5-O), 2,2′-(ethylenedioxy)diethanethiol (8-O), and tetra(ethylene glycol) dithiol (11-O)] and three alkanedithiols of corresponding length [1,5-pentanedithiol (5-C), 1,8-octanedithiol (8-C), and 1,11-undecanedithiol (11-C)]. All compounds were purchased from Sigma-Aldrich in the highest available purity grade and were used without additional purification.

Single Molecule Conductance (STM-Controlled Break Junction) Measurements. The conductance of the single dithiolated molecules was measured using the STM-controlled break-junction method.[2d] In this experiment, the molecules of interest are occasionally trapped between the substrate and an STM tip by periodic modulation of the tip−substrate separation. During this process, the tunneling current is monitored as a function of the tip−substrate distance at a constant bias voltage. The conductance is determined by analysis of the current−distance characteristics. All measurements were performed with an Agilent 5500 system equipped with an environmental chamber. The STM head was placed in a homemade, acoustically isolated Faraday cage, which was mounted on an active antivibrational system (Table Stable) located on an optical table. A brief description of the STM-BJ measurements is presented below.

Experiments were performed using freshly cut gold STM tips (0.25 mm, 99.999% gold wire, Alfa Aesar). Typically, 5−10 tips were used to collect sufficient data for each molecule. 100 nm thick gold films on silicon (Sigma-Aldrich) were used as the substrates. Typically, at least three independent substrates were used to collect 2000−3000 current−distance characteristics for each studied compound. Prior to the measurements, the substrates were cleaned for 10−20 s in piranha solution, rinsed solely with deionized water, and dried under a stream of argon. Measurements were performed in 2 mM solutions in mesitylene under an argon atmosphere. A 10 nA/V preamplifier was used in the measurements. Current−distance curves were recorded under 0.5 V bias. Curves that displayed current plateaus (20−30% of the total data set) were manually selected for further analysis. Measured conductances were plotted in the form of normalized histograms on a logarithmic scale, with 25 bins per decade. For each of the studied molecules, a Gaussian function was fitted to the conductance distribution to determine the position of the conductance peak. The conductance distributions are plotted on a linear scale together with the fitted Gaussian functions in the Supporting Information. Conductance results are expressed in the units of the quantum conductance, $G_0 = 2e^2/h \approx 77\ \mu S$.

In order to plot two-dimensional (2-D) conductance−displacement distributions, it is necessary to determine a zero distance in a constant and meaningful way. For each current−distance curve, the beginning of the drop of measured current from its maximum value of 100 nA ($\sim 2.5 \times 10^{-3}\ G_0$) was taken to define the zero of distance. This part of the curve represents the moment at which direct contact between the gold tip and gold substrate breaks, and thus the measured current rapidly decreases to zero. The distributions were built with a bin size in the displacement scale of 0.24 Å.

Theoretical Calculations of the Conductance. A nonequilibrium Green's function (NEGF) method, which has been verified in the weak coupling limit,[22] was employed to

dx.doi.org/10.1021/jp307902v | J. Phys. Chem. B 2013, 117, 4431−4441

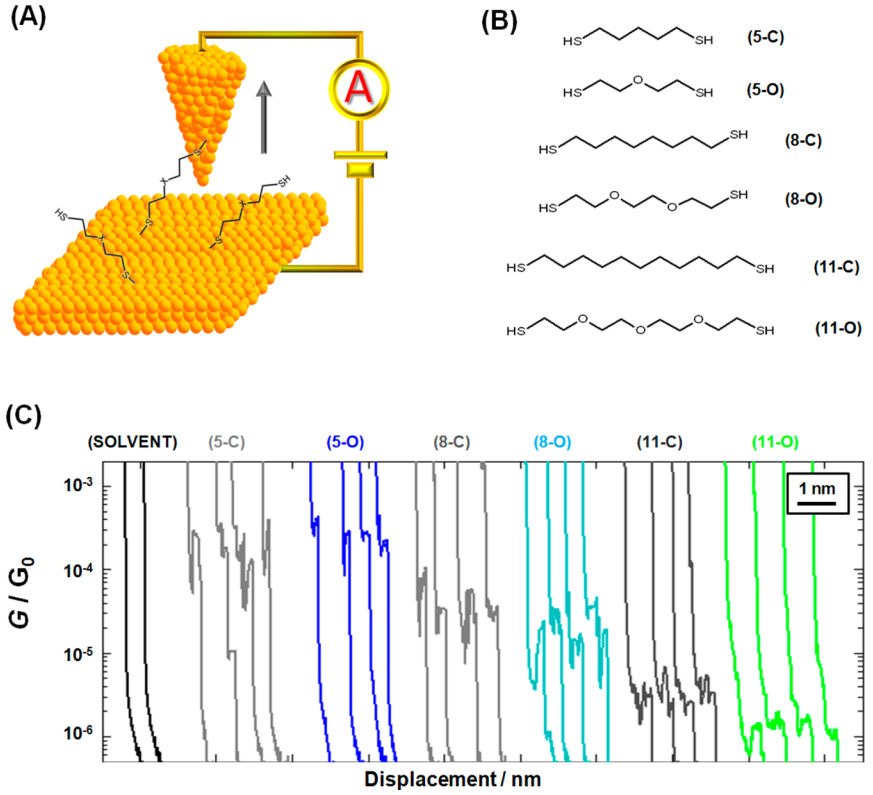

Figure 1. Panel A shows a cartoon representation of the STM break junction. Panel B shows the molecular structures of 1,5-pentanedithiol (5-C), 2-mercaptoethyl ether (5-O), 1,8-octanedithiol (8-C), 2,2′-(ethylenedioxy)diethanethiol (8-O), 1,11-undecanedithiol (11-C), and tetra(ethylene glycol) dithiol (11-O). Panel C shows sample conductance−distance curves recorded in the presence of the molecules in the junction. For comparison, typical curves recorded in pure mesitylene (solvent) are shown also.

calculate the conductance. First, the geometries of all six molecules were optimized at the RHF/6-31G(d) level using Gaussian 03.[23] Next, the Fock matrix from the last SCF calculation was transformed into a fully localized natural atomic orbital (NAO) basis[24] through Gaussian's NBO 3.1 routine[25] and used in the following Green's function:

$$G(\varepsilon) = \frac{1}{\varepsilon \mathbf{I} - \mathbf{F} - \mathbf{\Sigma}_L - \mathbf{\Sigma}_R} \tag{1}$$

where $\mathbf{F}$ is the NAO Fock matrix and ε is the energy variable. The self-energy matrix $\mathbf{\Sigma}$, which describes the molecular orbital (eigenstates of the NAO Fock matrix) broadening that arises from the coupling to left (L) and right (R) electrodes, was calculated using the broadening matrix $\mathbf{\Gamma}$ through $\mathbf{\Gamma} = i[\mathbf{\Sigma} - \mathbf{\Sigma}^+]$. The values of the matrix elements of $\mathbf{\Gamma}$ represent the coupling between corresponding NAOs and electrodes. A 0.1 eV electrode−NAO coupling strength, which is the same value used previously,[9e,22b] was set for the terminal sulfur NAOs. Because linkers are always present in experiments, the terminal carbon atoms were included in the broadening matrix to get the correct trend of conductance. The method for the weak coupling limit is optimized for model molecules without a "linker". For the models with linkers, the coupling was kept weak enough between the electrode and terminal carbon NAOs so that the molecular bridge states are not significantly perturbed. The transmission was computed by way of eq 2

$$T(\varepsilon) = Tr[\mathbf{\Gamma}_L \mathbf{G} \mathbf{\Gamma}_R \mathbf{G}^+] \tag{2}$$

and the conductance was calculated by way of Landauer's formula

$$\sigma = \frac{q^2}{h} \int T(\varepsilon) F_T(\varepsilon - E_F)\, d\varepsilon \tag{3}$$

where q is the elementary charge and h is Planck's constant. The function F_T is the difference between the Fermi functions of the left and right electrodes,[9e] namely,

$$F_T(\varepsilon - E_F) = \frac{1}{4k_BT} \operatorname{sech}^2\left(\frac{\varepsilon - E_F}{2k_BT}\right) \tag{4}$$

E_F is the Fermi level, which was set at −5.5 eV to reflect the value for Au.[26] Because of the strong decrease in the value of F_T as the energy ε moves away from E_F, the dominant contribution to the conductance σ is from $T(\varepsilon = E_F)$. By defining a scoring factor,[22a] the transmission (and the current) was decomposed into contributions from specific orbitals: $T(\varepsilon = E_F) = \sum_m SF_m$. The scoring factor is expressed as

$$SF_m = \sum_n \frac{\Gamma^L_{mm}\Gamma^R_{nm}}{(E_F - \varepsilon_m)(E_F - \varepsilon_n)} \tag{5}$$

in which Γ^L_{mn} and Γ^R_{nm} are the corresponding elements of matrices $\mathbf{\Gamma}_L$ and $\mathbf{\Gamma}_R$. ε_m is the energy of molecular orbital m.

RESULTS AND DISCUSSION

Single Molecule Conductance. The single molecule conductance is studied using the STM-BJ[2d] method, in which a gold STM tip serves as one electrode and the gold substrate serves as a second electrode of the junction (Figure 1A). During retraction of the tip from the substrate, the current is measured as a function of the distance between the electrodes.

dx.doi.org/10.1021/jp307902v | J. Phys. Chem. B 2013, 117, 4431−4441

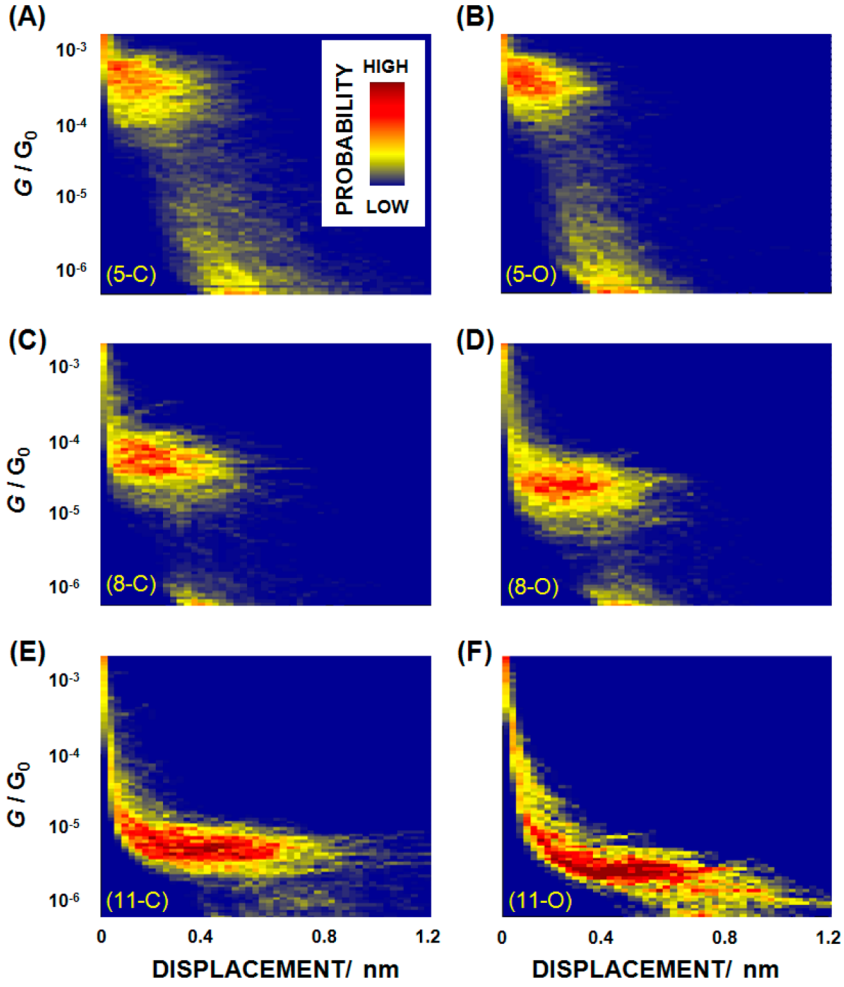

Figure 2. Two-dimensional conductance−displacement distributions are shown for 1,5-pentanedithiol (A), 2-mercaptoethyl ether (B), 1,8-octanedithiol (C), 2,2′-(ethylenedioxy)diethanethiol (D), 1,11-undecanedithiol (E), and tetra(ethylene glycol) dithiol (F). The color bar in panel A is common for all compounds.

In pure solvent, the current distance curves are well described by an exponential decay, such as the black curves presented in Figure 1C. If thiol functionalized molecules are present in the solvent, they can be trapped between the tip and the substrate and contribute to the overall conductance of the junction. Figure 1C shows sample experimental curves which display step-like features that arise from the conduction through molecule(s) that are trapped between the tip and the substrate. The differently colored traces in Figure 1C correspond to the different molecules that are studied in this work. The structures of the molecules are given in Figure 1B.

Because the conformations of the molecules and their binding geometries can vary, the measured conductance varies from trace to trace;[3c−e] nevertheless, its distribution is characteristic for each studied compound. Figure 2 shows two-dimensional conductance−displacement distributions constructed from the many conductance−distance curves recorded for each compound. The displacement axis reflects the distance at which the STM tip is withdrawn after the direct contact between the tip and the substrate is broken. Note that the length of the conductance steps in the conductance−distance characteristics represents the distance at which a particular junction can be stretched rather than the length of the molecules.[2d]

For each compound, the measured conductance varies by less than an order of magnitude, and the conductance for a family of compounds becomes smaller with increasing length of the molecule. The values of the conductances that are determined for the alkanedithiol chains (5-C, 8-C, and 11-C) are in good agreement with the values reported by others for the single molecule conductance of alkanedithiols[3d,e] (more details are provided in the Supporting Information). The average distances at which the junctions break are dependent on the length of the molecules, and it varies from 2 to 3 Å for 5-C and 5-O, to 3 to 5 Å for 8-C and 8-O, and 6 to 8 Å for 11-C and 11-O. Other than a shift in the conductance values of the steps, no significant difference in overall shape of the conductance−distance dependencies (Figure 1C) and in the average length of the conductance steps (Figure 2) are observed between the hydrocarbon and oligoether chains with the same number of bridge units (sum of $-CH_2$ and oxygen atoms in the chain). Furthermore, a comparison of the conductance distributions for the 5-C and 5-O chains shows very similar conductances for these two compounds. However, the situation changes when longer molecules, with a larger number of oxygen atoms in the chain, are compared with their hydrocarbon analogues.

Figure 3 shows a direct comparison between the conductance distributions constructed for alkanedithiol (5-C,

dx.doi.org/10.1021/jp307902v | J. Phys. Chem. B 2013, 117, 4431−4441

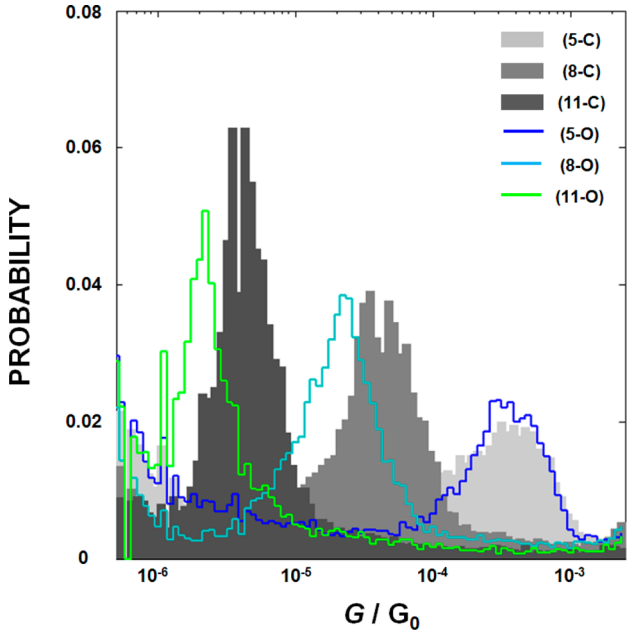

Figure 3. The plot compares the conductance distributions of dithiolated hydrocarbons (5-C, 8-C, 11-C) and oligoethers (5-O, 8-O, 11-O). The shaded distributions represent the hydrocarbon chains, and the colored curves sketch the distributions for the corresponding oligoethers (green is 11-O, aqua is 8-O, and blue is 5-O).

8-C, and 11-C) and oligoether (5-O, 8-O, and 11-O) molecules. Evaluation of the conductance distributions for 5-C and 5-O indicates that replacing a single carbon atom in the hydrocarbon chain by an oxygen reduces the average conductance of the chain by several percent. If each third methylene unit in the longer chain molecules is replaced by an oxygen (compounds 8-O and 11-O, see Figure 1B), the effect becomes stronger and leads to about a 50% decrease of the average conductance when compared to the hydrocarbon counterparts (8-C and 11-C). These conclusions assume that the S−Au contact geometry/configurations of the ether and alkane molecules are the same; in fact, the alkane results agree well with the "medium" conductance mode that has been identified by other workers[3e,18] (see the Supporting Information for a discussion) and the oligoether chain conductances agree well with those reported by Scullion et al. using the STM $I(s)$ method.[17] The increasing influence of the oxygen atoms on the conductance of the longer oligoether chains, which is observed in the single molecule conductance experiments, is supported by theoretical calculations with the NEGF method. Both measured and calculated conductances are given in Table 1.

Relationship between Electronic Structure and Calculated Conductance. Figure 4 compares the contributions of particular molecular orbitals (MOs) to the calculated conductance for the 8-C and 8-O molecules, by plotting scoring factors SF versus the molecular orbital index (top row in Figure 4).[22a] Because the values of scoring factors can be positive or negative, constructive and deconstructive interference between different MOs is important in determining the overall conductance of the molecule, which is proportional to the sum of all SFs (∑SFs). The bottom panel in Figure 4 compares the summation of SFs for occupied and unoccupied levels, beginning from the frontier molecular orbitals. That is, the sum is taken from the highest occupied molecular orbital (HOMO)

Table 1. The Average Experimental Conductance of Studied Compounds and the Calculated Conductance of the Model Compounds

	conductance, G_0	
molecule	measured	calculated[a]
5-C	$(4.6 \pm 2.9) \times 10^{-4}$	2.6×10^{-9}
5-O	$(4.2 \pm 2.3) \times 10^{-4}$	1.9×10^{-9}
(5-O/5-C)	0.91	0.74
8-C	$(5.2 \pm 2.5) \times 10^{-5}$	7.0×10^{-11}
8-O	$(2.5 \pm 1.2) \times 10^{-5}$	4.1×10^{-11}
(8-O/8-C)	0.48	0.59
11-C	$(4.7 \pm 1.9) \times 10^{-6}$	2.2×10^{-12}
11-O	$(2.1 \pm 0.7) \times 10^{-6}$	1.3×10^{-12}
(11-O/11-C)	0.45	0.58

[a]The NEGF methods used here are not expected to reproduce the absolute values of the experimental conductances for this system. Simplifications about the nature of the electrode−molecule coupling and the exact position of the metal Fermi levels can strongly shift the absolute values. The approach is believed to capture relative charge transport trends between systems, however.[9e,22]

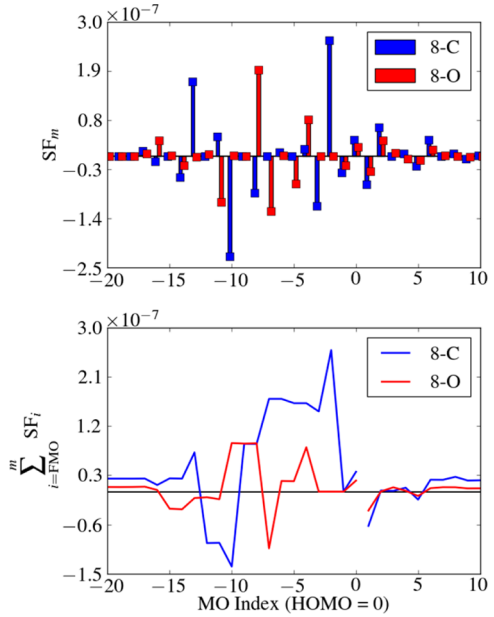

Figure 4. Comparison of scoring factors (top row) and their sums (bottom row) for 8-C (blue) and 8-O (red) molecules are plotted versus MO index. The sums are calculated separately for HOMO and LUMO levels starting from frontier molecular orbitals.

downward in energy, and a corresponding sum is taken from the lowest unoccupied molecular orbital (LUMO) upward in energy. Three major conclusions are drawn from this comparison: (i) SFs are typically higher for HOMOs than LUMOs, suggesting hole-mediated charge transfer, (ii) ∑SFs are higher for the alkane chains, as compared to the alkoxy chains, and (iii) for both alkoxy and alkyl chains, the contributions of particular MOs to the conductance become important below the HOMO-1 level. The comparisons of SFs and ∑SFs for these molecules plotted versus energy, and versus MO index, are given in the Supporting Information (Figures S4−S6).

Starting from the HOMO-2 level, the differences in SF values, and consequently in ∑SFs, become apparent with a high contribution of this level to the conductance of the 8-C

dx.doi.org/10.1021/jp307902v | J. Phys. Chem. B 2013, 117, 4431−4441

Table 2. Energies of Selected Molecular Orbitals for the Dithiol Molecules[a]

	energy (eV)					
molecular orbital	5-C	5-O	8-C	8-O	11-C	11-O
HOMO	−9.68	−9.83	−9.63	−9.81	−9.60	−9.80
HOMO-1	−9.69	−9.85	−9.63	−9.81	−9.60	−9.80
HOMO-2	−12.00	−11.96	−11.76	−11.74	−11.55	−11.64

[a]Note that the HOMO and HOMO-1 are primarily thiol nonbonding electrons (see text).

molecule, but a negligible value for 8-O. Table 2 gives some energies for some selected MOs with respect to the vacuum level. The differences in energy of levels listed in Table 2 are less than 0.2 eV in all molecules. In particular, the energy of the HOMO-2 level in 8-C and in 8-O is similar; thus, the molecular conductance of 8-C and 8-O cannot be explained exclusively by their orbital energetics.

Figure 5 shows the spatial distributions of selected MOs for 8-C and 8-O. One can see that the HOMO and HOMO-1 levels are fully localized at the terminal sulfur atoms, and are very similar for the alkyl and oligoether chains. This localization indicates little contribution from carbons on the bridge, and indicates that these orbitals can be viewed primarily as symmetric and antisymmetric combinations of the sulfur lone pair orbitals. The longer molecular bridge minimizes direct coupling between the two terminal atoms further. Together with the symmetry of these molecules, this leads to an interesting result that the HOMO and HOMO-1 levels are nearly degenerate and their total contributions to the conductance almost cancel each other in the weak coupling limit. This picture is consistent with model systems in which the terminal sulfur groups are attached to a gold atom or small gold clusters. In those cases, these orbitals would delocalize between the sulfur and gold atoms or clusters but would not contribute significantly to the charge density on the molecular bridge.[3e,27]

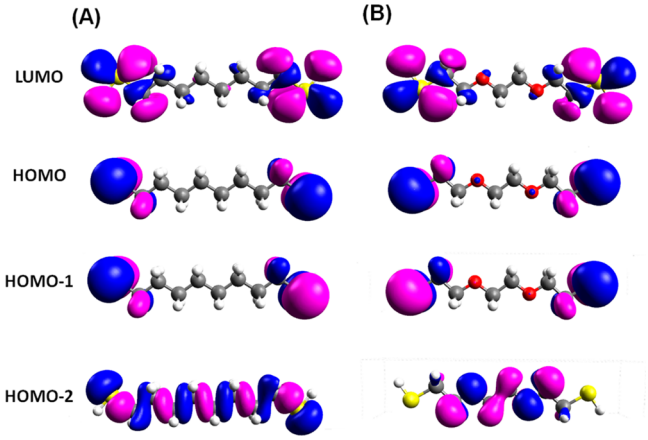

Figure 5. Spatial distributions are shown for selected molecular orbitals in 8-C (A) and 8-O (B).

The spatial distribution of probability amplitude for the HOMO-2 level in these molecules is qualitatively different. In the case of 8-C, the HOMO-2 orbital is delocalized along the entire molecule, while in the case of 8-O it is more localized on the oxygen atoms. Similar differences in the localization of the HOMO-2 levels have been found for the shorter and longer chains also; see Figure 6.

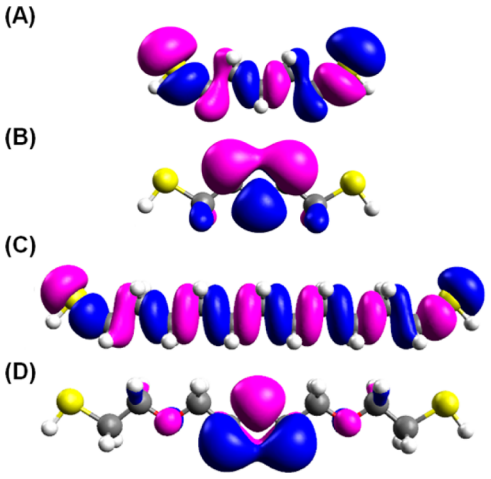

Figure 6. Spatial distributions of the HOMO-2 orbital are shown for 5-C (A), 5-O (B), 11-C (C), and 11-O (D). Spatial distributions of LUMO, HOMO, and HOMO-1 levels for these molecules can be found in the Supporting Information.

The degree of localization of the MOs was quantified by defining a normalized localization factor (NLF) for each MO. Because the MOs have been transformed into the natural atomic orbital (NAO) basis (*vide supra*), each MO can be decomposed into a linear combination of NAOs:

$$\mathrm{MO}_m = \sum_{i=1}^{n} c_{m,i}\mathrm{NAO}_i \tag{6}$$

where $c_{m,i}$ is a coefficient and $|c_{m,i}|^2$ is the contribution of the ith NAO to the mth MO. A localization factor for MO_m can be defined as the coefficient of variation of the corresponding MO coefficients:

$$\mathrm{LF}_m = \frac{\mathrm{std}(c_m)}{\langle c_m \rangle} \tag{7}$$

where $\mathrm{std}(c_m)$ is the standard deviation of the series of c_m and $\langle c_m \rangle$ is the mean. To compare molecules with a different number of NAOs, LF is normalized to its highest possible value for each molecular orbital and the normalized localization factor (NLF) is used in the following discussion.

$$\mathrm{NLF}_m = \frac{\mathrm{LF}_m}{\mathrm{LF}_{\max}} \tag{8}$$

The NLF values can vary between 0 and 1, where "0" means that the MO is fully delocalized (all of the chain's heavy atom orbitals contribute equally to the MO) and "1" means that the MO is localized on a single atomic orbital. Some of the calculated NLF values are presented in Table 3. The HOMO and HOMO-1 levels are strongly localized on the terminal sulfur atoms (see Figure 5), and the same high NLF value of 0.66 is calculated for these MOs in all the molecules. For both

dx.doi.org/10.1021/jp307902v | J. Phys. Chem. B 2013, 117, 4431−4441

Table 3. Normalized Localization Factors (NLFs) for Selected Molecular Orbitals

	molecular orbital				
molecule	HOMO-2	HOMO-1	HOMO	LUMO	filled states[a]
5-C	0.30	0.66	0.66	0.29	0.34
5-O	0.60	0.66	0.66	0.30	0.38
8-C	0.27	0.66	0.66	0.29	0.28
8-O	0.46	0.66	0.66	0.30	0.32
11-C	0.27	0.66	0.66	0.30	0.25
11-O	0.60	0.66	0.66	0.30	0.30

[a]The average NLF of all MOs formed from the valence atomic orbitals.

alkanes and oligoethers, the LUMO is delocalized along the chain; however, the contribution of this orbital to the overall conductance is small (see Figure 4 and Figures S4 and S5, Supporting Information) because of its position with respect to the Fermi level. On the other hand, NLF values calculated for the HOMO-2 show a strong difference in the localization. The oligoethers have NLF values that are nearly as high as that of the HOMO and HOMO-1,[28] whereas the alkyl chains show delocalization that is more similar to the LUMO orbitals. The contribution of each MO to the conductance (scoring factors) depends not only on the localization factor but also on the MO's energy relative to the Fermi level and on how much the terminal atomic orbital (which is coupled with the electrode) contributes to the MO. This feature suggests that the differences in the HOMO-2 are dominantly responsible for the differences in the conductances; however, other filled orbitals show a higher delocalization for the alkanes than the oligoethers. The last column in Table 3 reports the average NLF over all filled states, which shows the same trend.

Analysis of the Charge Transfer Pathways. Although the MO based conductance analysis explains the general trend, analyzing the MOs directly masks how the local bonding and site energy changes affect the conductance. To further explore these effects, a pathway analysis based on fully localized natural bond orbitals (NBOs)[11,20] is performed. Six symmetric, model molecules: $\bullet CH_2(CH_2)_3CH_2\bullet$, $\bullet CH_2CH_2OCH_2CH_2\bullet$, $\bullet CH_2(CH_2)_6CH_2\bullet$, $\bullet CH_2(CH_2OCH_2)_2CH_2\bullet$, $\bullet CH_2(CH_2)_9CH_2\bullet$, and $\bullet CH_2(CH_2OCH_2)_3CH_2\bullet$, are used as model donor-bridge-acceptor representations of 5-C, 5-O, 8-C, 8-O, 11-C, and 11-O molecules, respectively. The terminal radicals play the role of the donor or the acceptor for each model molecule. Terminal sulfurs are not included in order to explore better the molecular bridge charge transfer properties of the chains. Following Lewis,[16a] the single molecule conductance in the superexchange regime can be approximated as

$$\sigma = |V|^2 \frac{2\pi e^2}{\hbar}\left[\left(\frac{\pi}{6}\right)^{2/3}\frac{D_{m,L}l_{m,L}}{d_{m,L}{}^{2/3}}\frac{D_{m,R}l_{m,R}}{d_{m,R}{}^{2/3}}\right] \quad (9)$$

where V is the electronic coupling through the molecular bridge, D_m is the density of electronic states in the metal, d_m is the atomic density of the metal (atoms cm^{-3}), l_m is the effective coupling length of the bridge's wave function into the metal (in cm), and the R (L) index indicates the right (left) metal contact. The other symbols have their usual meanings. Because the electronic coupling is the only variable that depends on the molecular structure of the bridge, the conductance analysis is reduced to an electronic coupling analysis. The geometry and electronic structure of the triplet diradicals are calculated at the UHF/3-21G level using Gaussian 03,[23] which is accurate enough for this NBO analysis; see refs 11, 20, and 29. The Fock matrices obtained from the *ab initio* calculation are transformed into the NBO basis using Gaussian 03's NBO option.[25]

Both the radical cation coupling (dominated by hole-mediated superexchange) and radical anion coupling (dominated by electron-mediated superexchange) can be determined from the neutral molecule NBO Fock matrix, when combined with Koopmans theorem.[30,31] The general procedure is to diagonalize the α and β NBO Fock matrices, from which the splitting of the α HOMO and HOMO-1 levels corresponds to $2|V|$ for the radical cation and the splitting of the β LUMO and LUMO+1 levels corresponds to $2|V|$ for the radical anion; see Figure 7. If all elements of the NBO Fock matrix are retained, then the splittings are the same as the ones obtained from the original canonical molecular orbitals, because the change of basis does not affect the eigenvalues. The couplings obtained in this way are presented in Table 4 and labeled as "(full)". The

Table 4. Electronic Couplings (in cm^{-1}) for the Radical Cations and Anions

	5-C	5-O	8-C	8-O	11-C	11-O
$\|V\|_{cation}$(full)	4451	4238	1560	1172	613	333
$\|V\|_{anion}$(full)	4587	5349	940	1326	202	339
$\|V\|_{cation}$(only valence orbitals)	4517	4334	1715	1265	733	378
$\|V\|_{anion}$(only valence orbitals)	5479	6568	1223	1814	299	532

trend of $|V|_{cation}$(full) reproduces the experimental conductance trends: (i) ether chains have lower conductance than the corresponding alkyl chains; and (ii) the coupling difference

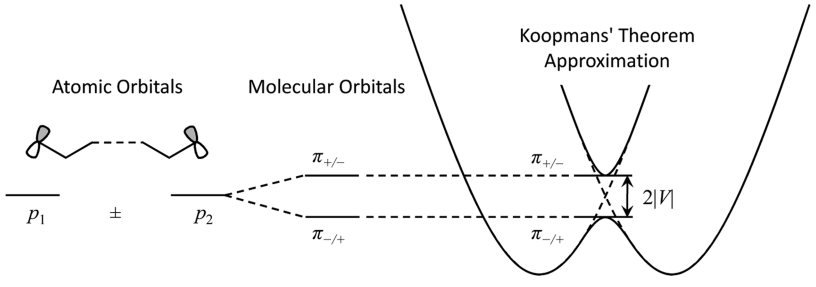

Figure 7. This schematic diagram shows how the electronic coupling relates to the orbital splitting. The two unpaired electrons (shown here as p atomic orbitals) form frontier molecular orbitals (FMOs) that can be labeled as "+" or "−" based on their parities. The sign of the splitting depends on the order of the two FMOs, and we follow the convention defined in ref 30.

dx.doi.org/10.1021/jp307902v | J. Phys. Chem. B 2013, 117, 4431−4441

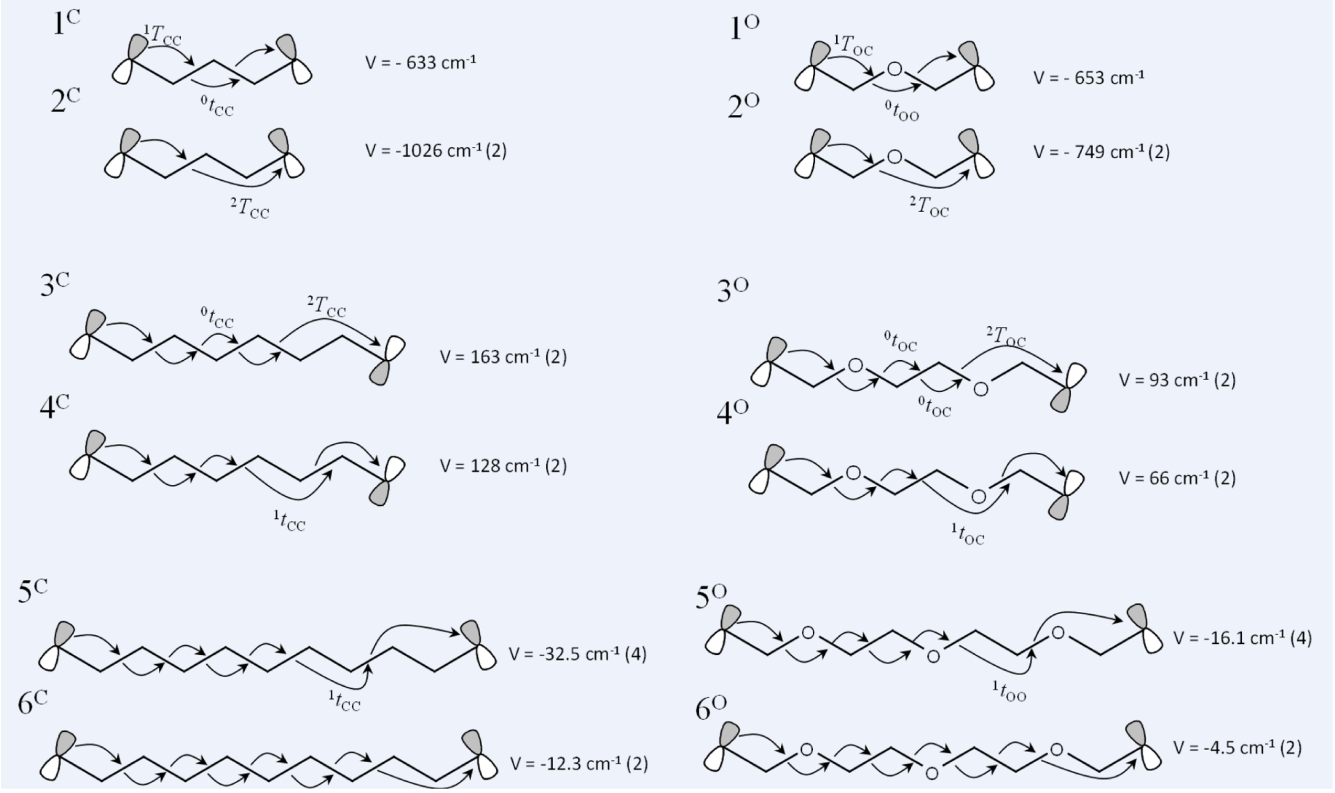

Figure 8. The diagrams show the dominant coupling pathways for the diradical model molecules. Couplings of identical pathways are combined together, and the number of the pathways is indicated in parentheses.

between 5-C and 5-O is much smaller than the difference between the longer chains. Although $|V|_{anion}$ and $|V|_{cation}$ are almost the same for the shortest chain molecules, one must consider their energy level position with respect to the Fermi level to ascertain the relative importance of electron-mediated pathways versus hole-mediated pathways. The actual Fermi level is much closer to the filled molecular orbitals, which should make the hole-mediated charge-transfer more favorable. This inference is supported by the conductance calculation and the scoring factor analysis which show that the hole-mediated superexchange dominates the coupling.

The benefit of the NBO pathway analysis arises from the use of a "reduced" NBO Fock matrix. The NBO basis set can be divided into "occupied" core orbitals, bonding orbitals (C−C, C−O, or C−H σ bonds in our system), and nonbonding lone-pair orbitals (the two terminal radicals; note the occupancy is one per orbital instead of two), "unoccupied" antibonding and extra-valence-shell orbitals (Rydbergs). The diagonal elements of the NBO Fock matrix correspond to the self-energy of each orbital, and the off-diagonal elements correspond to the interaction between the orbitals. By setting the corresponding off-diagonal elements to zero, one obtains a reduced Fock matrix with certain interactions turned off. The reduced Fock matrix can be treated in the same way as the full matrix to calculate a $|V|$ that retains only the desired interactions. The last two rows in Table 4 show such calculations for the cation radical case where interactions involving core orbitals and unoccupied orbitals are zeroed out, so that $|V|$ only contains the interactions among valence orbitals. Those values are similar to the corresponding "full" coupling, suggesting that the core orbitals and unoccupied orbitals play a minor role in the conductance. This finding is consistent with the earlier MO analysis and validates this approach. Note that the error for the anion coupling is larger than that for the cation coupling, because the unoccupied molecular orbitals are used in the anion cases, and they contain more contribution from the unoccupied NBOs in the full Fock matrix. Because the anion pathways are less important than the cation pathways, this feature is neglected. The discussion below focuses on $|V|_{cation}$ and valence orbitals.

The NBO Fock matrix of valence orbitals can be further reduced to retain only the interactions of NBOs on a specific coupling pathway, and the $|V|_{cation}$ can be decomposed into a set of couplings for individual pathways. This calculation is similar to the scoring factor decomposition of the conductance that was discussed above but from a more "local" perspective. The number of all possible pathways for all six molecules is too large to analyze one by one, but for the bridge length regime studied in this work, "forward" pathways through the C−C (and C−O for ether chains) backbone capture the main features of $|V|_{cation}$.[30−32] Figure 8 shows the dominant forward pathways for each of the six model molecules. The pairwise couplings are very similar from one matrix to another because of the portability of NBO interactions. The symbol T indicates the coupling element involving a donor or acceptor, and t is used for coupling interactions only involving backbone sigma bonds. Following the convention defined in ref 30, the superscript indicates the distance between the two NBOs with 0 corresponding to the nearest-neighbors. The subscript indicates the atom types, O for O−C and C for C−C in each bond. Note that the terminal lone pair orbital is perpendicular to the nearest σ bond so ${}^0T$ is usually very small and ${}^1T$ can be viewed as the *de facto* "nearest-neighbor" interaction. The signs of V come from the parity of the MOs and whether the symmetric

dx.doi.org/10.1021/jp307902v | J. Phys. Chem. B 2013, 117, 4431−4441

level is higher than the antisymmetric level. As observed previously,[11,32c] backbone only pathways are found to be constructive.

From Figure 8, it is clear that the nearest neighbor pathway which is used in McConnell's model (see below) is no more important than other non-nearest neighbor pathways, and it will become less and less important to the overall conductance as the chain length increases because of the rapid growth of the total number of non-nearest pathways.[32c] Another notable fact is that the McConnell pathways, 1^C and 1^O, have similar couplings, while the couplings of non-nearest pathways, such as $4^C/4^O$ and $5^C/5^O$, are always larger for alkyl chains as compared to ether chains. Thus, the larger number of possible non-nearest neighbor pathways and their dominant contribution to the overall charge transport in the longer chains (8-C, 8-O, and 11-C, 11-O) can explain the larger conductance difference between the longer alkane and ether chains than in the short chains, such as 5-C and 5-O.

Perturbation theory can be used to quantify this finding. The perturbation treatment decomposes the coupling strength of a pathway into the individual steps through the approximate expression[21]

$$V = \frac{\prod_{\mathrm{Dn}}^{\mathrm{Acc}} H_{i,j}}{\prod_{\mathrm{Bd}} \Delta_i} \tag{10}$$

$H_{i,j}$ represents the coupling between adjacent NBOs, starting from the NBO of the donor to the NBO of the acceptor through the σ bond NBOs of the chain. Δ_i is defined as $\Delta_i = \varepsilon_i - \varepsilon_{\mathrm{Dn}}$ in which ε_i is the self-energy of the NBOs and $\varepsilon_{\mathrm{Dn}}$ is the self-energy of the lone pair NBO of the donor (which is equal to the self-energy of the lone pair NBO of the acceptor). If only the nearest-neighbor pathway is considered, the analysis reduces to the original McConnell superexchange model.[33] Because of the portability of NBO, the averaged values for the same type of interaction were used; see Table 5. All the parameters in Table 5 are normalized to the corresponding C−C bonds only interactions. The results of the perturbation treatment based on Table 5 are listed in Table 6.

Table 5. Values of the Normalized Parameters Used in the Perturbation Calculations

subscript	Δ	^1T	^2T	^0t	^1t
CC	1	1	1	1	1
OC	1.52	0.99	1.09	0.94	0.88
OO				2.06	1.09

Table 6. Relative Couplings That Were Calculated Using the Perturbation Method for the Most Dominant Charge Transfer Pathways Compared with the Results Obtained Using MO Splittings

pathway[a]	(no. $^0t_{OO}$)/(no. Δ_{OC})[b]	V_O/V_C(perturbation)	V_O/V_C
1^O	0.5	0.91	1.03
2^O	0	0.73	0.73
3^O	0.33	0.58	0.57
4^O	0.33	0.50	0.52
5^O	0.4	0.59	0.50
6^O	0.4	0.47	0.37

[a]The labels refer to the diagrams in Figure 8. [b]Numbers of NBO interactions of each type in every pathway (see Figure 8) are tabulated in Table S1 in the Supporting Information.

As Table 6 shows, this analysis predicts a decrease in the ratio of V_O to V_C as the chain length increases, in qualitative agreement with the experiment. Note that the errors are larger for the last two long pathways, which is probably caused by the accumulated deviation between the average values and the actual values of the NBO couplings.

The interactions in the last two rows of Table 5 can be divided into two types which compensate each other: Type I interactions decrease the coupling compared to alkyl chains, and type II interactions increase the coupling compared to alkyl chains. Δ_{OC} is the strongest type I interaction; however, others will play a role in the final coupling when a lot of them are included (that is, when the chain length is long enough). The strong "self-energy effect" (Δ_{OC}) can be compensated by type II interactions, of which $^0t_{OO}$ is the strongest. The effects compensate most when the ratio of the number of $^0t_{OO}$ couplings and the number of the self-energy differences Δ_{OC} is as large as possible (see Table 6). The largest compensation exists for the 1^O pathway; thus, the overall coupling is close to that of 1^C. In contrast, when non-nearest neighbor pathways that skip a C−O bond are present, then the ratio will decrease. Although $^1t_{OO}$ and other type II interactions can compensate, they are minor as compared to $^0t_{OO}$. The non-nearest neighbor pathways for 8-C/O and 11-C/O are much more important than those for 5-C/O. Also, type I interactions other than Δ_{OC} begin to play a role. The overall effect is that the conductance/that the coupling difference is larger in long chains, such as 8-C/O and 11-C/O, than in the short chains, 5-C/O.

The pathway analysis, which is described above, only focuses on the $|V|_{\mathrm{cation}}$ in Table 4. If $|V|_{\mathrm{cation}}$ is taken to be the only electronic coupling in the system, then the large electronic coupling difference for longer chains is similar to what Napper et al. found $|V|_{\mathrm{cation}}(O)/|V|_{\mathrm{cation}}(C) \approx 0.6$ for a chain with 13 heavy atoms and one oxygen atom maximum),[11] but it is an overestimation when compared with the conductance experiments and calculation. This overestimation may result from not including the electron mediated $|V|_{\mathrm{anion}}$ in this latter analysis and suggests that hole-mediated tunneling may be more important in the electrochemical charge transfer than in the conductance measurements.

CONCLUSIONS

Single molecule conductance measurements of alkanes and their corresponding oligoethers show that the molecular conductance of oligoether chains is smaller than that of alkane chains. Computational methods are used to show that the contribution of the molecular orbitals to the conductance depends strongly on their delocalization, with higher contributions for more delocalized orbitals. Delocalization of the orbitals is found to be higher in the alkyl chains than in the oligoethers, a trend that is in agreement with that of the conductances determined experimentally. In addition, an NBO pathway analysis shows that the self-energy shift of the C−O is compensated by an increased coupling for the shortest chains, 5-C and 5-O. For the longer chains, the non-nearest neighbor contributions to the overall coupling decrease this compensation and the difference in couplings through the two chains is more strongly manifested.

ASSOCIATED CONTENT

Supporting Information

Conductance distributions are plotted on a linear scale with fitted Gaussian functions; comparison of conductance meas-

dx.doi.org/10.1021/jp307902v | J. Phys. Chem. B 2013, 117, 4431−4441

ured for alkanedithiols with published data; conductance−length dependences; scoring factors; and spatial distributions of selected molecular orbitals. This material is available free of charge via the Internet at http://pubs.acs.org.

AUTHOR INFORMATION

Corresponding Author

*E-mail: dave@pitt.edu.

Notes

The authors declare no competing financial interest.

ACKNOWLEDGMENTS

D.H.W. acknowledges support from the National Science Foundation (CHE 1057981). We thank K. D. Jordan (U. Pittsburgh) for useful discussions during the study, and we thank R. Nichols (U. Liverpool) for helpful comments. Computational resources were provided by the Center for Simulation and Modeling at the University of Pittsburgh.

REFERENCES

(1) (a) Mann, B.; Kuhn, H. *J. Appl. Phys.* **1971**, *42*, 4398−4405. (b) Aviram, A.; Ratner, M. A. *Chem. Phys. Lett.* **1974**, *29*, 277−283.

(2) (a) Reed, M. A.; Zhou, C.; Muller, C. J.; Burgin, T. P.; Tour, J. M. *Science* **1997**, *278*, 252−254. (b) Porath, D.; Bezryadin, A.; de Vries, S.; Dekker, C. *Nature* **2000**, *403*, 635−638. (c) Cui, X. D.; Primak, A.; Zarate, X.; Tomfohr, J.; Sankey, O. F.; Moore, A. L.; Moore, T. A.; Gust, D.; Harris, G.; Lindsay, S. M. *Science* **2001**, *294*, 571−574. (d) Xu, B.; Tao, N. J. *Science* **2003**, *301*, 1221−1223. (e) Guo, X.; Small, J. P.; Klare, J. E.; Wang, Y.; Purewal, M. S.; Tam, I. W.; Hong, B. H.; Caldwell, R.; Huang, L.; O'Brien, S.; et al. *Science* **2006**, *311*, 356−359.

(3) (a) Haiss, W.; Nichols, R. J.; van Zalinge, H.; Higgins, S. J.; Bethell, D.; Schiffrin, D. J. *Phys. Chem. Chem. Phys.* **2004**, *6*, 4330−4337. (b) Venkataraman, L.; Klare, J. E.; Tam, I. W.; Nuckolls, C.; Hybertsen, M. S.; Steigerwald, M. L. *Nano Lett.* **2006**, *6*, 458−462. (c) Wierzbinski, E.; Slowinski, K. *Langmuir* **2006**, *22*, 5205−5208. (d) Li, X.; He, J.; Hihath, J.; Xu, B.; Lindsay, S. M.; Tao, N. *J. Am. Chem. Soc.* **2006**, *128*, 2135−2141. (e) Li, C.; Pobelov, I.; Wandlowski, T.; Bagrets, A.; Arnold, A.; Evers, F. *J. Am. Chem. Soc.* **2007**, *130*, 318−326. (f) Martín, S.; Giustiniano, F.; Haiss, W.; Higgins, S. J.; Whitby, R. J.; Nichols, R. J. *J. Phys. Chem. C* **2009**, *113*, 18884−18890. (g) Parameswaran, R.; Widawsky, J. R.; Vázquez, H.; Park, Y. S.; Boardman, B. M.; Nuckolls, C.; Steigerwald, M. L.; Hybertsen, M. S.; Venkataraman, L. *J. Phys. Chem. Lett.* **2010**, *1*, 2114−2119.

(4) (a) Huber, R.; González, M. T.; Wu, S.; Langer, M.; Grunder, S.; Horhoiu, V.; Mayor, M.; Bryce, M. R.; Wang, C.; Jitchati, R.; et al. *J. Am. Chem. Soc.* **2007**, *130*, 1080−1084. (b) Yamada, R.; Kumazawa, H.; Noutoshi, T.; Tanaka, S.; Tada, H. *Nano Lett.* **2008**, *8*, 1237−1240. (c) Kaliginedi, V.; Moreno-García, P.; Valkenier, H.; Hong, W.; García-Suárez, V. M.; Buiter, P.; Otten, J. L. H.; Hummelen, J. C.; Lambert, C. J.; Wandlowski, T. *J. Am. Chem. Soc.* **2012**, *134*, 5262−5275. (d) Diez-Perez, I.; Hihath, J.; Hines, T.; Wang, Z.-S.; Zhou, G.; Mullen, K.; Tao, N. *Nat. Nanotechnol.* **2011**, *6*, 226−231.

(5) Morita, T.; Lindsay, S. *J. Phys. Chem. B* **2008**, *112*, 10563−10572.

(6) (a) Shih, K.-N.; Huang, M.-J.; Lu, H.-C.; Fu, M.-D.; Kuo, C.-K.; Huang, G.-C.; Lee, G.-H.; Chen, C.-h.; Peng, S.-M. *Chem. Commun.* **2010**, *46*, 1338−1340. (b) Zhou, X.-S.; Liu, L.; Fortgang, P.; Lefevre, A.-S.; Serra-Muns, A.; Raouafi, N.; Amatore, C.; Mao, B.-W.; Maisonhaute, E.; Schoellhorn, B. *J. Am. Chem. Soc.* **2011**, *133*, 7509−7516.

(7) (a) Sedghi, G.; Sawada, K.; Esdaile, L. J.; Hoffmann, M.; Anderson, H. L.; Bethell, D.; Haiss, W.; Higgins, S. J.; Nichols, R. J. *J. Am. Chem. Soc.* **2008**, *130*, 8582−8583. (b) Kiguchi, M.; Takahashi, T.; Kanehara, M.; Teranishi, T.; Murakoshi, K. *J. Phys. Chem. C* **2009**, *113*, 9014−9017. (c) Perrin, M. L.; Prins, F.; Martin, C. A.; Shaikh, A. J.; Eelkema, R.; van Esch, J. H.; Briza, T.; Kaplanek, R.; Kral, V.; van Ruitenbeek, J. M.; et al. *Angew. Chem. Int. Ed.* **2011**, *50*, 11223−11226. (d) Li, Z.; Park, T.-H.; Rawson, J.; Therien, M. J.; Borguet, E. *Nano Lett.* **2012**, *12*, 2722−2727.

(8) (a) Xiao, Xu; Tao. *J. Am. Chem. Soc.* **2004**, *126*, 5370−5371. (b) Sek, S.; Misicka, A.; Swiatek, K.; Maicka, E. *J. Phys. Chem. B* **2006**, *110*, 19671−19677.

(9) (a) Xu, Z.; Li, T. *Nano Lett.* **2004**, *4*, 1105−1108. (b) Hihath, J.; Xu, B.; Zhang, P.; Tao, N. *Proc. Natl. Acad. Sci. U.S.A.* **2005**, *102*, 16979−16983. (c) van Zalinge, H.; Schiffrin, D. J.; Bates, A. D.; Haiss, W.; Ulstrup, J.; Nichols, R. J. *ChemPhysChem* **2006**, *7*, 94−98. (d) Wierzbinski, E.; Arndt, J.; Hammond, W.; Slowinski, K. *Langmuir* **2006**, *22*, 2426−2429. (e) Venkatramani, R.; Davis, K. L.; Wierzbinski, E.; Bezer, S.; Balaeff, A.; Keinan, S.; Paul, A.; Kocsis, L.; Beratan, D. N.; Achim, C.; et al. *J. Am. Chem. Soc.* **2011**, *133*, 62−72. (f) Wierzbinski, E.; de Leon, A.; Davis, K. L.; Bezer, S.; Wolak, M. A.; Kofke, M. J.; Schlaf, R.; Achim, C.; Waldeck, D. H. *Langmuir* **2012**, *28*, 1971−1981.

(10) Thuo, M. M.; Reus, W. F.; Simeone, F. C.; Kim, C.; Schulz, M. D.; Yoon, H. J.; Whitesides, G. M. *J. Am. Chem. Soc.* **2012**, *134*, 10876−10884.

(11) Napper, A. M.; Liu, H.; Waldeck, D. H. *J. Phys. Chem. B* **2001**, *105*, 7699−7707.

(12) Cheng, J.; Saghi-Szabo, G.; Tossell, J. A.; Miller, C. J. *J. Am. Chem. Soc.* **1996**, *118*, 680−684.

(13) (a) Chidsey, C. E. D.; Bertozzi, C. R.; Putvinski, T. M.; Mujsce, A. M. *J. Am. Chem. Soc.* **1990**, *112*, 4301−4306. (b) Paul, A.; Watson, R. M.; Lund, P.; Xing, Y.; Burke, K.; He, Y.; Borguet, E.; Achim, C.; Waldeck, D. H. *J. Phys. Chem. C* **2008**, *112*, 7233−7240.

(14) (a) Sek, S.; Misicka, A.; Bilewicz, R. *J. Phys. Chem. B* **2000**, *104*, 5399−5402. (b) Sek, S.; Palys, B.; Bilewicz, R. *J. Phys. Chem. B* **2002**, *106*, 5907−5914. (c) Wain, A. J.; Do, H. N. L.; Mandal, H. S.; Kraatz, H.-B.; Zhou, F. *J. Phys. Chem. C* **2008**, *112*, 14513−14519.

(15) Slowinski, K.; Chamberlain, R. V.; Miller, C. J.; Majda, M. *J. Am. Chem. Soc.* **1997**, *119*, 11910−11919.

(16) (a) Traub, M. C.; Brunschwig, B. S.; Lewis, N. S. *J. Phys. Chem. B* **2007**, *111*, 6676−6683. (b) Venkatramani, R.; Wierzbinski, E.; Spiros, S. S.; Borguet, E.; Achim, C.; Waldeck, D. H.; Beratan, D. N. To be submitted for publication, 2012. (c) Wierzbinski, E.; Venkatramani, R.; Davis, K. L.; Bezer, S.; Kong, J.; Xing, Y.; Borguet, E.; Achim, C.; Beratan, D. N.; Waldeck, D. H. Under review, 2012.

(17) Scullion, L. E.; Leary, E.; Higgins, S. J.; Nichols, R. J. *J. Phys.: Condens. Matter* **2012**, *24*, 164211.

(18) General conclusions arising from the conductance measurements may be incorrect if one of the S−Au contact geometries is less likely to be observed in alkoxy chains than in alkanes; e.g., two groups of contact geometries exist for them, instead of the three groups reported for alkyl chains (Li et al. *J. Am. Chem. Soc.* **2008**, *130*, 318). As a result, different groups of the conductance (low, medium, or high) for different types of molecules would be compared with each other. Nevertheless, we do not find a physical reason for why the number of medium/low conductance events would be different for alkyl and alkoxy chains.

(19) (a) Leary, E.; Hoebenreich, H.; Higgins, S. J.; van Zalinge, H.; Haiss, W.; Nichols, R. J.; Finch, C. M.; Grace, I.; Lambert, C. J.; McGrath, R.; et al. *Phys. Rev. Lett.* **2009**, *102*, 086801. (b) Li, X.; Hihath, J.; Chen, F.; Masuda, T.; Zang, L.; Tao, N. *J. Am. Chem. Soc.* **2007**, *129*, 11535−11542. (c) Cao, H.; Jiang, J.; Ma, J.; Luo, Y. *J. Am. Chem. Soc.* **2008**, *130*, 6674−6675.

(20) Jordan, K. D.; Paddon-Row, M. N. Electron Transfer Calculations. In *Encyclopedia of Computational Chemistry*; John Wiley & Sons: New York, 1998.

(21) Ratner, M. A. *J. Phys. Chem.* **1990**, *94*, 4877−4883.

(22) (a) Paul, A.; Bezer, S.; Venkatramani, R.; Kocsis, L.; Wierzbinski, E.; Balaeff, A.; Keinan, S.; Beratan, D. N.; Achim, C.; Waldeck, D. H. *J. Am. Chem. Soc.* **2009**, *131*, 6498−6507. (b) Wierzbinski, E.; de Leon, A.; Yin, X.; Balaeff, A.; Davis, K. L.; Rappireddy, S.; Venkatramani, R.; Keinan, S.; Ly, D. H.; Madrid, M.; et al. *J. Am. Chem. Soc.* **2012**, *134*, 9335−9342.

(23) Frisch, M. J.; Trucks, G. W.; Schlegel, H. B.; Scuseria, G. E.; Robb, M. A.; Cheeseman, J. R.; Montgomery, J. A., Jr.; Vreven, T.;

Kudin, K. N.; Burant, J. C.; et al. *Gaussian 03*, revision E.01.; Gaussian, Inc.: Wallingford, CT, 2004.
(24) (a) Reed, A. E.; Weinhold, F. *J. Chem. Phys.* **1983**, *78*, 4066−4073. (b) Reed, A. E.; Weinstock, R. B.; Weinhold, F. *J. Chem. Phys.* **1985**, *83*, 735−746.
(25) Glendening, E. D.; Reed, A. E.; Carpenter, J. E.; Weinhold, F. *NBO*, version 3.1. See ref 23.
(26) Ashcroft, N. W.; Mermin, N. D. *Solid state physics*; Harcourt College Publishers: New York, 1976.
(27) Haiss, W.; Martin, S.; Scullion, L. E.; Bouffier, L.; Higgins, S. J.; Nichols, R. J. *Phys. Chem. Chem. Phys.* **2009**, *11*, 10831−10838.
(28) The difference in the NLF factors for the HOMO-2 of 8-O and the HOMO-2 of the 5-O, 11-O arises from the differences in the symmetry of the 8-O (C2h) and 5-O/11-O (C2v) molecules.
(29) Shephard, M. J.; Paddon-Row, M. N.; Jordan, K. D. *Chem. Phys.* **1993**, *176*, 289−304.
(30) Liang, C.; Newton, M. D. *J. Phys. Chem.* **1992**, *96*, 2855−2866.
(31) Liang, C.; Newton, M. D. *J. Phys. Chem.* **1993**, *97*, 3199−3211.
(32) (a) Curtiss, L.; Naleway, C.; Miller, J. *J. Phys. Chem.* **1993**, *97*, 4050−4058. (b) Curtiss, L. A.; Naleway, C. A.; Miller, J. R. *Chem. Phys.* **1993**, *176*, 387−405. (c) Jordan, K. D.; Paddon-Row, M. N. *Chem. Rev.* **1992**, *92*, 395−410. (d) Shephard, M. J.; Paddon-Row, M. N.; Jordan, K. D. *J. Am. Chem. Soc.* **1994**, *116*, 5328−5333.
(33) McConnell, H. M. *J. Phys. Chem.* **1961**, *35*, 508−515.